

See discussions, stats, and author profiles for this publication at: <https://www.researchgate.net/publication/256934818>

# Natural motion of one-dimensional flexible objects using minimization approaches

**Article** in Mechanism and Machine Theory · September 2013  
DOI: 10.1016/j.mechmachtheory.2013.04.003

CITATIONS  
8

READS  
48

3 authors:



**Midhun S Menon**  
Indian Institute of Science  
7 PUBLICATIONS 16 CITATIONS

SEE PROFILE



**G. K. Ananthasuresh**  
Indian Institute of Science  
208 PUBLICATIONS 3,190 CITATIONS


SEE PROFILE



**Ashitava Ghosal**  
Indian Institute of Science  
122 PUBLICATIONS 1,327 CITATIONS

SEE PROFILE

Some of the authors of this publication are also working on these related projects:

 Resolution of redundancy [View project](#)

 SERIUS, CSP-2 [View project](#)

# Natural motion of one-dimensional flexible objects using minimization approaches

Midhun S. Menon\*, G. K. Ananthasuresh<sup>†</sup> and Ashitava Ghosal<sup>‡</sup>  
Dept. of Mechanical Engineering  
Indian Institute of Science  
Bangalore 560 012, India

## Abstract

For one-dimensional flexible objects such as ropes, chains, hair, the assumption of constant length is realistic for large-scale 3D motion. Moreover, when the motion or disturbance at one end gradually dies down along the curve defining the one-dimensional flexible objects, the motion appears “natural”. This paper presents a purely geometric and kinematic approach for deriving more natural and length-preserving transformations of planar and spatial curves. Techniques from variational calculus are used to determine analytical conditions and it is shown that the velocity at any point on the curve must be along the tangent at that point for preserving the length and to yield the feature of diminishing motion. It is shown that for the special case of a straight line, the analytical conditions lead to the classical tractrix curve solution. Since analytical solutions exist for a tractrix curve, the motion of a piece-wise linear curve can be solved in closed-form and thus can be applied for the resolution of redundancy in hyper-redundant robots. Simulation results for several planar and spatial curves and various input motions of one end is used to illustrate the features of motion damping and eventual alignment with the perturbation vector.

**Keyword:** Flexible body simulation, Length-preserving natural motion, Optimization, Tractrix, Hyper-redundant robots.

## 1 Introduction

Simulation of motion of one-dimensional flexible objects and their realistic and natural visual display is an active area of research. Such a problem is encountered in the simulation and visualization of motion of objects such as a rope or human hair. In such situations, for a given pre-defined motion of the *leading* end, the motion of the *trailing parts* need to be computed and displayed as realistically as possible. Since there exist infinite number of ways in which the trailing parts can move, practically feasible strategies, resulting in visually and otherwise realistic motions, are required to obtain a trajectory of the trailing parts. This problem has received much attention in the last few decades and there exists a large amount of literature on this topic [1]. More recent interest in surgery training, where flexible suturing thread is modeled as spring-mass-damper systems [2, 3], is related to this problem. In these works, the equations of motion are solved to predict the motion of parts

---

\*Graduate Student. Email: midhun.sreekumar@gmail.com

<sup>†</sup>Email: suresh@mecheng.iisc.ernet.in

<sup>‡</sup>Corresponding author. E-mail: asitava@mecheng.iisc.ernet.in, Tel. +91 80 2293 2956

of the rope. A major difficulty in this approach is that there is no systematic way of choosing the spring, damping and other parameters. In another approach [4], Cosserat theory of elastic rods is applied to solve the problem. In yet another attempt [5], key-framing techniques are used without considering the kinematics or dynamics that govern the motion. However, most of these methods lack uniqueness in formulation and realism in the simulated motion produced.

The problem of simulation of one-dimensional objects has its parallel in hyper-redundant manipulators and robots where the inverse kinematics problem does not have a unique solution – for a given motion of the end-effector, there exist infinitely many solutions for the joint variables. Choosing a useful/meaningful solution from the feasible space is known as resolution of redundancy and there exist several approaches to solve this problem. The most well-known methods involve minimization of an objective function of the joint velocities (using the pseudo-inverse of the manipulator Jacobian matrix) (see, the review paper by Klein and Huang [6], textbook by Nakamura [7] and works by Liegeois [8], Baillieul et al. [9] and Yoshikawa [10]), modeling and obtaining the motion of a backbone/spine curve [11, 12], and the use of the classical tractrix curve<sup>1</sup>, originally by Reznik and Lumelsky [14, 15, 16] and more recently by Sreenivasan et al. [17] and by Ravi et al. [18]. In the conventional tractrix curve-based approach, the entire flexible object is discretized into a finite number of rigid (straight) segments connected with imaginary revolute/spherical joints. For a prescribed motion of the *head* of the leading segment, the motion of the *trailing* end of the same segment is computed by employing the analytical solution of the differential equation of a tractrix. One key property of a tractrix, making it a very promising candidate for realistic motion simulation of one-dimensional flexible objects, is that for a given motion of the leader, the motions of the trailing parts die down or attenuates as one moves away from the perturbed end. An additional well-known property of the tractrix is that the velocity of the trailing end is along the line joining the trailing and the leading end. More importantly, this velocity is the *least* among all possible velocities of the trailing end of the object for a given motion of the leading end. This suggests that the tractrix-based solution can be obtained from a general minimization problem.

In this paper, we revisit and extend the notion of length preservation and velocity minimization to arbitrary planar and spatial curves modeling one-dimensional flexible objects. Using formal tools from calculus of variations, we minimize the  $L_2$  norm between two configurations of a curve subject to the length preservation constraint. We show that, for any planar or spatial curve subject to preservation of the length, the  $L_2$  norm gets minimized when the velocity of any point on the curve is along the tangent at that point. For the special case of a straight line, we show that the results are identical to the classical tractrix solution. Subsequently, by means of a limiting argument, we prove that for a arbitrary curve, the motion dies out as one moves away from the perturbed end and the effect of the motion or disturbance is localized. We also show that when the perturbation is along a straight line the entire curve, independent of its initial shape, deforms and eventually aligns with the perturbation and becomes a straight line. Both these features results in a more “natural” looking motion of the curve and the flexible one-dimensional object modeled by the curve. Finally, we also demonstrate that other metrics such as the angular motion (i.e., the bending of the flexible object) and stiffness can also be minimized and each of these minimization lead to different unique solutions.

The paper is organized into six sections. For the sake of completeness, we present the motion of a single straight rigid body, the associated concept of a tractrix and present its key properties in Section 2. In Section 3, we use calculus of variation to derive analytical results dealing with the motion of an arbitrary curve. It is shown that the general results yield the tractrix solution when the curve is a straight line. Subsequently, an algorithm to simulate the motion of a flexible object modeled as a curve or as a piece-wise linear segments is presented. In Section 4, other

---

<sup>1</sup>According to Steinhaus [13], the tractrix is *the path traced by an object starting off with a vertical offset when it is dragged along by a string of constant length being pulled along a straight horizontal line*. The tractrix curve was studied by the great mathematician Leibniz, who obtained the differential equation and analytical solution of the curve.

metric functions which could also be used for minimization are presented. The simulation results are described and discussed in Section 5. The concluding remarks are in Section 6.

## 2 The tractrix formulation

Consider a rigid rod  $AP$  of length  $L$  initially lying along the  $Y$  axis as shown in figure 1. Let the end  $P$ , the *leading end*, be pulled along the  $X$  axis. Let  $A_1P_1$  denote an arbitrary configuration of the rigid rod. Without any constraint on the motion of end  $A$ , i.e., the *trailing end*, it can trace an arbitrary curve in the  $X - Y$  plane. For example,  $A$  can move *parallel* to the  $X$  axis and this

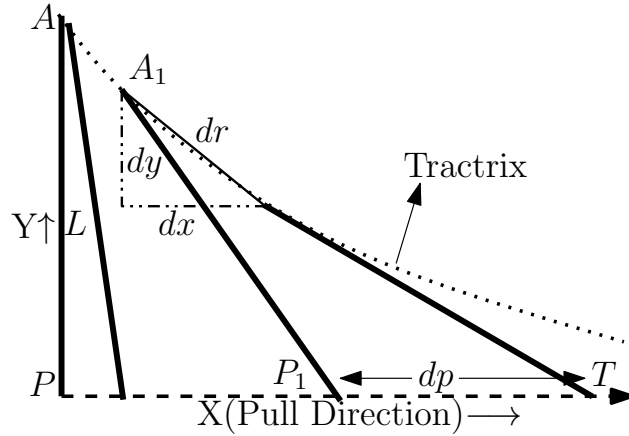


Figure 1: Motion of link  $AP$  when leading end  $P$  is pulled along  $PT(X\text{-Axis})$

corresponds to a *pure translation* of the rod. Now consider a constraint that the velocity *is along the rod at every instant*. Under such a constraint, the motion of point  $A$  can be described by the ordinary differential equation

$$\frac{dy}{dx} = \frac{-y}{\sqrt{L^2 - y^2}} \quad (1)$$

where  $(x, y)$  are the coordinates of point  $A$  and the denominator  $\sqrt{L^2 - y^2}$  arises from using the length preservation constraint  $x^2 + y^2 = L^2$ .

Equation (1) has a closed-form solution [13] given by

$$x = L \log \frac{y}{L - \sqrt{L^2 - y^2}} - \sqrt{L^2 - y^2} \quad (2)$$

which in terms of a parameter  $p$  can be written as

$$x(p) = p - L \tanh\left(\frac{p}{L}\right), \quad y(p) = L \operatorname{sech}\left(\frac{p}{L}\right) \quad (3)$$

The curve described by equations (2) or (3), traced by the end  $A$ , is called the tractrix and this curve is known to have several interesting properties. We list some of the main ones.

- The magnitude of the instantaneous velocity of  $A$  is the minimum of all possible velocities when  $A$  traces the tractrix. This follows from the following reasoning:

From elementary mechanics, the velocity of  $A$  can be written as

$$\mathbf{V}_A = \mathbf{V}_P + \omega \times \overrightarrow{PA} \quad (4)$$

where  $\omega$  is the angular velocity and  $\overrightarrow{PA}$  denotes the vector from  $P$  to  $A$  with magnitude  $L$ . From equation (4) it follows that  $|\mathbf{V}_A| \leq |\mathbf{V}_P| + |\omega \times \overrightarrow{PA}|$  and  $0 < |\mathbf{V}_A| \leq |\mathbf{V}_P|$ . The equality holds if  $\omega$  is zero, i.e., when the rigid body is lying on the  $X$  axis and  $\mathbf{V}_A$  is parallel to  $\mathbf{V}_P$ .

Denoting the infinitesimal motion of  $A$  by  $dr$  and the motion of  $P$  by  $dp$  (shown in figure 1), we can write  $dr \leq dp$  (refer [17] for an alternate algebraic proof).

- The position of  $A$  or the trailing end can be obtained in closed-form in terms of hyperbolic functions as shown in equation (3).
- The motion of  $P$  need not be along the  $X$  axis or in the plane. The formulation can be extended to motion along any direction and in 3D (for details see [17, 18]).

The above properties were first used by Reznik and Lumelsky [14, 15, 16] for resolution of redundancy in hyper-redundant serial robots. In their work, for a desired motion of the end-effector or leading end, the motion of the trailing end was computed. The computed trailing end motion was used as the desired motion of the previous link and thus recursively, the motion of all links, down to the first link, was computed. In comparison to the pseudo-inverse and modal approaches mentioned earlier, the strategy led to a more natural motion since due to  $dr \leq dp$ , the motion of the links of the hyper-redundant robot tends to *die out* as one moves from the end-effector to the fixed base. In addition, the redundancy resolution is in *task space variables* and is of *linear complexity*. More recently Sreenivasan et al. [17] used the tractrix based approach to simulate and visualize more natural motion of snakes and ropes, and Ravi et al. [18] experimentally demonstrated the more natural motion on a planar eight-link hyper-redundant robot.

In the next section, we present an extension of the minimization of motion of a (rigid) straight line segment to arbitrary continuous (flexible) curves in a plane and 3D by using tools from calculus of variation.

### 3 Optimizing motion of a continuous curve

Consider a planar curve of length  $L$ , parametrized by its arc length  $s$ , and one of its end is given a prescribed motion. As shown in figure 2, the arbitrary motion of one end is assumed to be given by two independent continuous functions  $(T_x(t), T_y(t))$ . The curve at any instant  $t$  can be written in terms of a spatio-temporal parametrization as

$$C : (T_x(t) + x(s, t), T_y(t) + y(s, t)) \quad (5)$$

The terms  $(x(s, t), y(s, t))$  define the curve configuration relative to the perturbed tip, i.e., the curve configuration when viewed from a moving coordinate system attached to the perturbed tip. Note that, in this proposed parametrization, the functions  $x(0, t) = 0$  and  $y(0, t) = 0$  at any instant  $t$ . This is due to the fact that at  $s = 0$  (leading end), the absolute displacements are completely specified by the predefined functions  $(T_x(t), T_y(t))$ .

For the infinitesimal displacement shown in figure 2 from time  $t$  to  $t + \Delta t$ , the “distance”<sup>2</sup> between the two curves can be defined as

$$L_2 : \int_0^L \sqrt{\left(\frac{dT_x}{dt} + \frac{\partial x(s, t)}{\partial t}\right)^2 + \left(\frac{dT_y}{dt} + \frac{\partial y(s, t)}{\partial t}\right)^2} ds \quad (6)$$

---

<sup>2</sup>The defined *metric* is not a measure of distance between two rigid body configurations – such a metric does not exist as has been shown by Angeles [19]. The quantity is a *pseudo metric* to indicate the *closeness* of two curves of the same length. For a straight line, we show in Section 3.1 that this metric is related to the minimization of velocity of the points on the straight line.

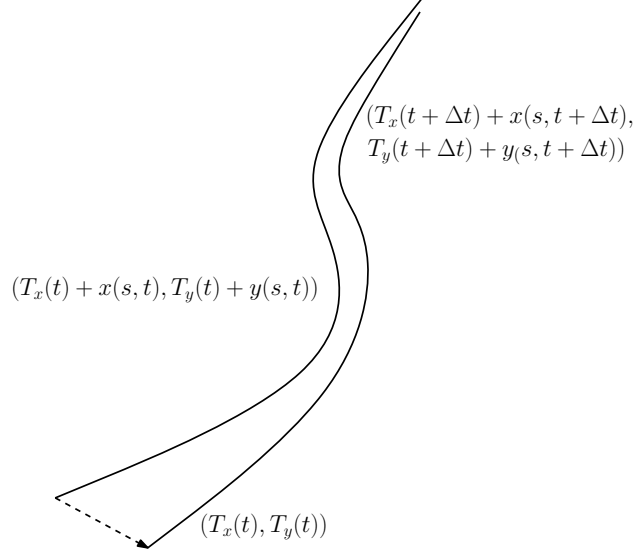


Figure 2: Infinitesimally displaced configurations along with perturbation function

The metric defined above is called the  $L_2$  metric due to its similarity with the Euclidean distance.

We also wish to impose the constraint that the length of the curve is preserved during the motion, and this can be written as

$$\int_0^L \left( \sqrt{\left( \frac{\partial x(s, t)}{\partial s} \right)^2 + \left( \frac{\partial y(s, t)}{\partial s} \right)^2} - 1 \right) ds = 0 \quad (7)$$

The variational problem now reduces to one of minimization of the  $L_2$  metric till a specified time  $T$  and can be stated as follows:

$$\begin{aligned} \text{Min } I_{x(s, t), y(s, t)} &: \int_0^L \int_0^T \sqrt{\left( \frac{dT_x}{dt} + \frac{\partial x(s, t)}{\partial t} \right)^2 + \left( \frac{dT_y}{dt} + \frac{\partial y(s, t)}{\partial t} \right)^2} dt ds \\ \text{Subject to} & \\ \Lambda(t) : A &= \int_0^L \left( \sqrt{\left( \frac{\partial x(s, t)}{\partial s} \right)^2 + \left( \frac{\partial y(s, t)}{\partial s} \right)^2} - 1 \right) ds = 0 \\ \text{Data} &: x(s, 0), y(s, 0), T_x(t), T_y(t), x(0, t) = 0, y(0, t) = 0 \end{aligned} \quad (8)$$

where  $\Lambda(t)$  is the Lagrangian multiplier corresponding to the length-preserving constraint. The Lagrangian for the above optimization, is written as

$$\mathcal{L} = I + \Lambda(t)A \quad (9)$$

and the corresponding Euler-Lagrange equations [20, 21] are as follows:

$$\frac{\partial \mathcal{L}}{\partial x} - \frac{\partial}{\partial s} \left( \frac{\partial \mathcal{L}}{\partial x'} \right) - \frac{\partial}{\partial t} \left( \frac{\partial \mathcal{L}}{\partial \dot{x}} \right) = 0 \quad (10a)$$

$$\frac{\partial \mathcal{L}}{\partial y} - \frac{\partial}{\partial s} \left( \frac{\partial \mathcal{L}}{\partial y'} \right) - \frac{\partial}{\partial t} \left( \frac{\partial \mathcal{L}}{\partial \dot{y}} \right) = 0 \quad (10b)$$

Note that  $x' = \frac{\partial}{\partial s}x(s, t)$  and  $\dot{x} = \frac{\partial}{\partial t}x(s, t)$  and similar notations are used for the variable  $y(s, t)$ . By using equations (10a) and (10b), and eliminating the Lagrange multiplier  $\Lambda(t)$  by division, we obtain the following:

$$\frac{\frac{\partial}{\partial s}y(s, t)}{\frac{\partial}{\partial s}x(s, t)} = \frac{\frac{d}{dt}T_y(t) + \frac{\partial}{\partial t}y(s, t)}{\frac{d}{dt}T_x(t) + \frac{\partial}{\partial t}x(s, t)} = \frac{\frac{\partial}{\partial t}(T_y(t) + y(s, t))}{\frac{\partial}{\partial t}(T_x(t) + x(s, t))} \quad (11)$$

Though quantitative results are specific to the equation of the assumed curve, i.e, choice of  $(x(s, t), y(s, t))$ , qualitatively, we can make the following *general* and *key* observations.

- The Lagrange multiplier has the units of velocity and this can be shown as follows:

The Euler-Lagrange equations (10a) and (10b) can be written as

$$\Lambda(t)y'\kappa_s = -(\dot{y} + \dot{T}_y(t))\kappa_t \quad (12)$$

$$-\Lambda(t)x'\kappa_s = (\dot{x} + \dot{T}_x(t))\kappa_t \quad (13)$$

where  $\kappa_s$  and  $\kappa_t$  are given by

$$\begin{aligned} \kappa_s &= \frac{x'y'' - y'x''}{(x'^2 + y'^2)^{\frac{3}{2}}} \\ \kappa_t &= \frac{(\dot{x} + \dot{T}_x(t))(\ddot{y} + \ddot{T}_y(t)) - (\dot{y} + \dot{T}_y(t))(\ddot{x} + \ddot{T}_x(t))}{((\dot{x} + \dot{T}_x(t))^2 + (\dot{y} + \dot{T}_y(t))^2)^{\frac{3}{2}}} \end{aligned} \quad (14)$$

Squaring and adding equations (12) and (13), and simplifying, we get

$$\Lambda(t)\kappa_s = \kappa_t V \quad (15)$$

where  $V = \sqrt{(\dot{T}_x + \dot{x})^2 + (\dot{T}_y + \dot{y})^2}$  is the velocity at any point on the curve. Hence, it is clear that the Lagrange multiplier has units of velocity.

- The extreme left-hand side of (11) is the spatial derivative or the slope at a given  $s$  and  $t$  and the far right-hand side is the temporal derivative or the velocity vector for a given  $s$  and  $t$ . This implies for the curve, the  $L_2$  metric as defined in equation (6) *is minimized if the velocity vector at any  $(s, t)$  is along the tangent at that point*. In addition, during this minimizing motion, *the arc length of the curve is preserved*.

### 3.1 The special case of a straight line

For the special case when the curve is a straight rigid link and the input perturbation is along the  $X$  axis with the perturbed end on the  $X$  axis initially, the perturbation functions in equation (11) take the form:

$$\frac{d}{dt}T_x(t) = 1, \quad T_y(t) = 0 \quad (16)$$

Since the curve  $(x(s, t), y(s, t))$  is a straight line, we have

$$x(s, t) = a(t)s, \quad y(s, t) = b(t)s \quad (17)$$

and since the length of the curve  $L$  is preserved, we get

$$\sqrt{(aL - 0)^2 + (bL - 0)^2} = L \Rightarrow a^2 + b^2 = 1 \quad (18)$$

Furthermore, by assuming that the straight rigid link is vertical at  $t = 0$ , we get  $a(0) = 0$  &  $b(0) = 1$ . Under the aforementioned conditions, the straight line equations transform as

$$x(s, t) = a(t)s + t, \quad y(s, t) = b(t)s \quad (19)$$

and we also have

$$a^2 + b^2 = 1 \Rightarrow 2a \frac{da}{dt} + 2b \frac{db}{dt} = 0 \Rightarrow \frac{db}{dt} = -\frac{a}{b} \frac{da}{dt} \quad (20)$$

Finally, substituting the above in the (11), and simplifying, we get

$$\begin{aligned} \frac{b}{a} &= \frac{db/dt \ s}{1 + da/dt \ s} = \frac{-\frac{a}{b} \frac{da}{dt} s}{1 + \frac{da}{dt} s} \Rightarrow s \frac{da(t)}{dt} + (1 - a(t)^2) = 0 \\ \Rightarrow a(t) &= -\tanh\left(\frac{t + K}{s}\right) \quad (K = \text{integration constant}) \end{aligned} \quad (21)$$

Using the initial conditions, we get  $K = 0$ , and

$$\begin{aligned} x(s, t) &= s\left(\frac{t}{s} - \tanh\left(\frac{t}{s}\right)\right) \\ y(s, t) &= s \operatorname{sech}\left(\frac{t}{s}\right) \end{aligned} \quad (22)$$

The path (curve) traced by the tip of the link is obtained by substituting  $s = L$  in the above equation. Denoting the perturbation in time  $t$  with  $p$ , we get

$$\begin{aligned} x(L, p) &= p - L \tanh\left(\frac{p}{L}\right) \\ y(L, p) &= L \operatorname{sech}\left(\frac{p}{L}\right) \end{aligned} \quad (23)$$

It can be seen that equation (23) is the same as that of a *tractrix* given in equation (3). The above derivation shows analytically that *for a straight single link perturbed along a straight line, the  $L_2$  metric (as defined in equation (6)) is equivalent to minimizing the velocity of the trailing end.*

As  $p \rightarrow \infty$  (or  $t \rightarrow \infty$ ), we know from elementary calculus that  $\tanh(p/L) \rightarrow 1$  and  $\operatorname{sech}(p/L) \rightarrow 0$  which gives

$$x(L, \infty) = p - L, \quad y(L, \infty) = 0 \quad (24)$$

From the above, it is clear that *as time increases, the straight line or the rigid link aligns with the perturbation direction*, in this case the  $X$ -axis.

### 3.2 Curve discretised by straight lines

It has not been possible to obtain analytical solution for equation (11) except for a simple straight line as shown in the preceding section. One way to solve the problem for an arbitrary curve is to discretise the curve into *finite number of straight line segments*. The difference between the continuous (variational) formulation and the discretised formulation is schematically shown in figure 3.

In Section 3.1, we demonstrated that for a straight line the motion of the trailing end with  $L_2$  metric or velocity minimization is given by the tractrix equations (23). As shown in the right-hand side of figure 3, a known perturbation is given to the 1<sup>st</sup> point (the leading end) of the initial



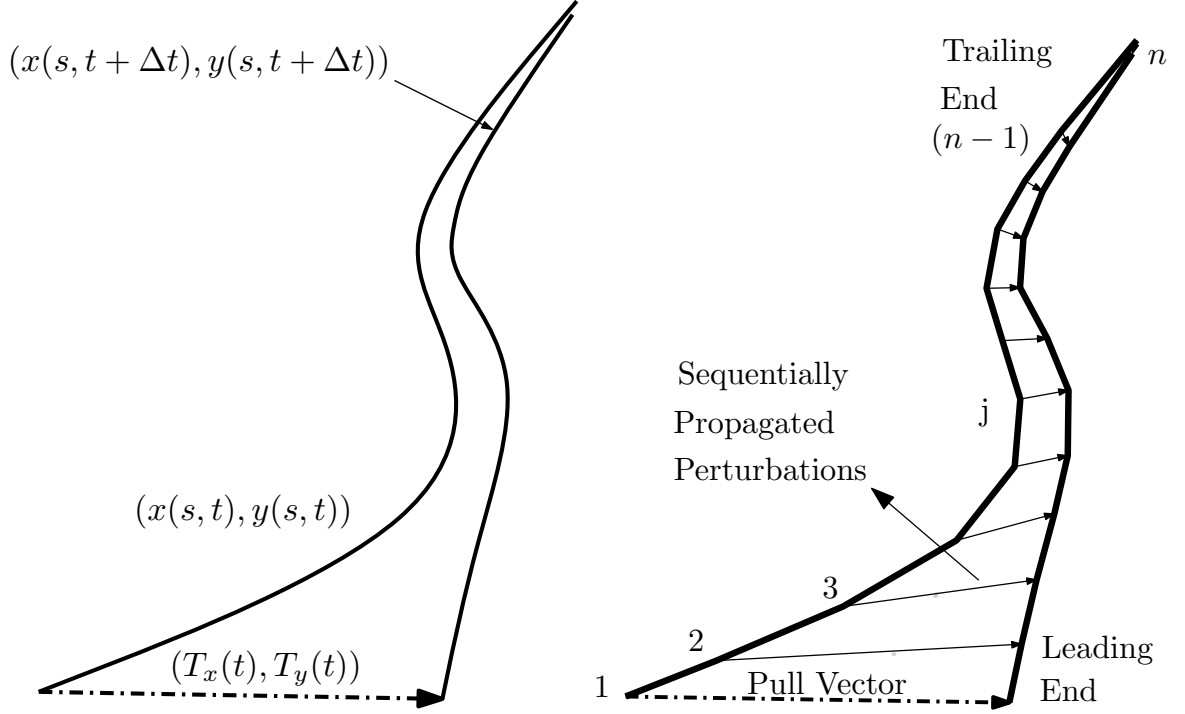


Figure 3: Difference between variational and discretized formulations

curve. The  $L_2$  metric minimizing the motion of trailing end of the 1<sup>st</sup> segment is computed in closed-form with equation (23) and this is the perturbation for the leading end of the 2<sup>nd</sup> segment. Sequential iteration along the linear segments up to the other end, generates the motion of the entire discretised curve or the  $n^{\text{th}}$  point. This approach is termed as sequential optimization and is the same as the strategy used for resolution of redundancy in hyper-redundant robots (see [14, 15, 16] and [17, 18]). Since for every iteration  $dr \leq dp$ , the perturbations die down as one moves down the segments and this gives a more ‘natural motion’ of the curve. In addition, to this ‘dying down’ or attenuation property, as shown in equation (24), as time progresses, the motion of each segment and hence the curve aligns with the motion of the perturbed end.

In giving the motion of the leading end in time domain, we have two options – either a single step in time from zero to  $T$  or a series of steps in time. The series of steps is to be used if the given perturbation is large or along a curve. For realistic simulations, the full step needs to be broken into several smaller steps. The first method is called the single-step optimization and the second is called the multi-step optimization. The multi-step optimization is more accurate when compared to the single step because, in the latter, we neglect the intermediate path points and consider only the initial and final states, which induces error. In the former case, we simply need to use the single step (tractrix approach) several time between  $t$  and  $(t + \Delta t)$  with  $\Delta t$  determined by the requirements of the simulation.

### 3.3 Spatial motion

For motion in 3D space, we can define the  $L_2$  metric (as a direct extension of the 2D  $L_2$  metric from equation 6) minimization as follows:

$$\begin{aligned}
& \underset{x(s), y(s), z(s)}{\text{Min } I} : \int_0^L \int_0^T \sqrt{\left(\frac{dT_x}{dt} + \frac{\partial x(s, t)}{\partial t}\right)^2 + \left(\frac{dT_y}{dt} + \frac{\partial y(s, t)}{\partial t}\right)^2 + \left(\frac{dT_z}{dt} + \frac{\partial z(s, t)}{\partial t}\right)^2} dt ds \\
& \text{Subject to} \\
& \Lambda(t) : A = \int_0^L \sqrt{\left(\frac{\partial x(s, t)}{\partial s}\right)^2 + \left(\frac{\partial y(s, t)}{\partial s}\right)^2 + \left(\frac{\partial z(s, t)}{\partial s}\right)^2} ds = L \\
& \text{Data : } x(s, 0), y(s, 0), z(s, 0), T_x(t), T_y(t), T_z(t), x(0, t) = 0, y(0, t) = 0, z(0, t) = 0
\end{aligned} \tag{25}$$

One can solve the optimization problem numerically<sup>3</sup> by discretizing the curve into piecewise straight lines. In Section 5, we present several numerical simulation results for the motion of curves in 2D and 3D. The interesting features of preservation of the length, dying-out of motion and eventual aligning of the curve along the perturbation is discernible in the simulations and accompanying animation files.

## 4 Use of other metrics for minimization

In the previous section, we presented a metric that expresses minimization of velocities of the trailing end for a given input velocity of a leading end. In this section, we present two additional possible metrics. In Section 5, we compare these metrics.

### 4.1 Minimization of body rotation

Consider a straight rigid segment  $AP$  and the leading end  $P$  is moved to point  $Q$ . We wish to obtain the motion of the trailing end  $A$  such that the straight rigid segment rotates the least. In figure 4, point  $A$  is schematically shown to move to  $B$  and hence the rotation angle is given by  $\angle BQR$  where line  $QR$  is parallel to  $AP$ .

We now pose a minimization problem:

$$\begin{aligned}
& \underset{x_B, y_B}{\text{Minimize : }} |(\angle BQR)| \\
& \text{Subject to : } |BQ| = L \\
& \text{Data : } L, \text{ Step Length } PQ
\end{aligned}$$

It may be noted that minimization of the rotation is in the same spirit as the  $L_2$  velocity minimization discussed in the previous section. Since a general rigid body motion can be considered to be a combination of translation and rotation, a solution of the above problem in combination with the tractrix approach may result in more natural rigid-body motions. It may be also noted that a curve can be discretised into straight rigid segments and the technique of sequential optimization can then be applied for the discretised body.

---

<sup>3</sup>In this work, numerical solution of optimization problems is done using the *fmincon* routine in MATLAB®[22].

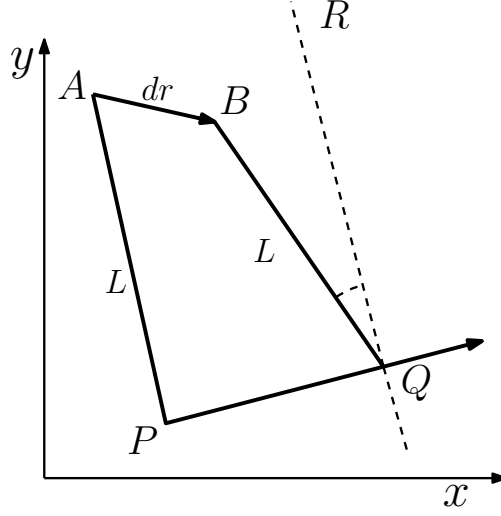


Figure 4: Incremental rotation minimization

## 4.2 Minimization of body deformation

Consider a rigid body comprising of two rigid line segments  $MA$  and  $AP$ . The end  $P$  is again given a perturbation to  $Q$ . We wish to determine the motion of  $A$  and  $M$ , schematically shown going to  $B$  and  $N$  respectively in figure 5, such that the  $(\angle MAP - \angle NBQ)$  is minimized. This can again be expressed as a minimization problem as follows:

$$\begin{aligned} \text{Minimize : } & |(\angle MAP - \angle NBQ)| \\ & x_B, y_B \\ \text{Subject to : } & |BQ| = L, |NB| = L \\ \text{Data : } & L, \text{ Step Length } PQ \end{aligned}$$

The above minimization indirectly determines the torsional stiffness between segments  $MA$  and  $AP$ .

## 5 Results and Discussion

In this section, we present numerical simulations to illustrate the theoretical results presented in the previous sections. All symbolic computations required for the results were obtained using MAPLE<sup>®</sup> [23] and for numerical simulations using the *fmincon* routine of MATLAB<sup>®</sup> [22].

### 5.1 Performance comparison of different optimization strategies

The first simulation result deals with a comparison of optimizing the motion of a continuous curve (discretised into piecewise linear segments) with the sequential, single and multi-step, optimization discussed earlier. As noted in Section 3, we can solve the continuous optimization for simple curves. Figure 6 shows the motion of an initial parabola using different optimization strategies. The chosen initial parabola has the form  $y = x^2$  and it is discretized into 20 segments, each of length 0.25 thereby creating a total curve length of 5. Further, for single-step perturbation, we have a pull vector of 0.7 length equally inclined to  $X$  and  $Y$  axes ( $45^\circ$  with each axis) whereas for the multi-step perturbation, we pull the curve in the same direction but in 5 steps of 0.14 each.

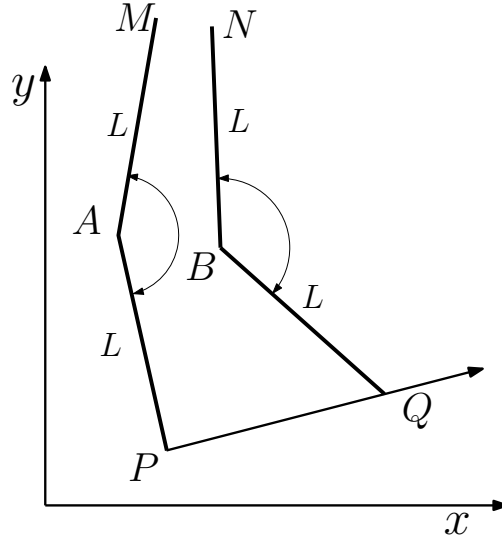


Figure 5: Incremental joint rotation minimization

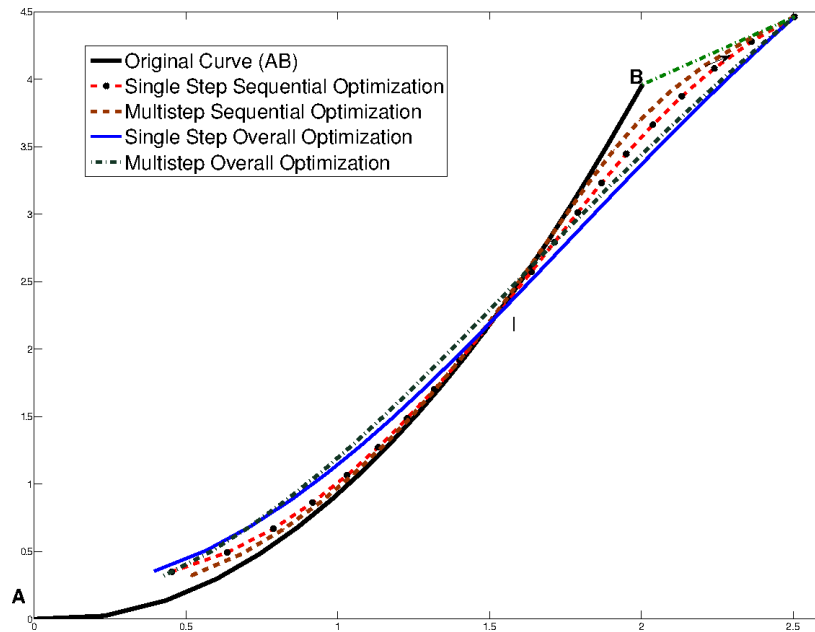


Figure 6: Different optimization techniques applied on an initial parabolic curve

To compare the four minimizations, we choose the multi-step sequential optimization as the reference. For single-step sequential optimization, the  $L_2$  norm is 0.6347 and for multi-step overall optimization the value is 1.6007 whereas for single-step overall optimization, it turns out to be 1.6982. This implies that better results are obtained if the discretization in time and along the curve is finer.

## 5.2 Solution characteristics of other candidate metrics and their significance

The second set of numerical results deals with the comparison of the tractrix, the minimization of body rotation and body deformation for a straight line. As explained earlier, selecting appropriate metrics depends greatly on the problem-specific task. In this section, the solution properties for the three metrics used in this paper are discussed.

1. The  $L_2$  norm minimization yields a tractrix-based solution as already mentioned earlier and shown in figure 7. It may be noted that the initial configuration of the straight line is parallel to the  $Y$  axis, the motion is from right to left, and the final configuration of the straight line is parallel to the  $X$  axis. The figure clearly demonstrates that the final configuration is aligned along the pull direction.

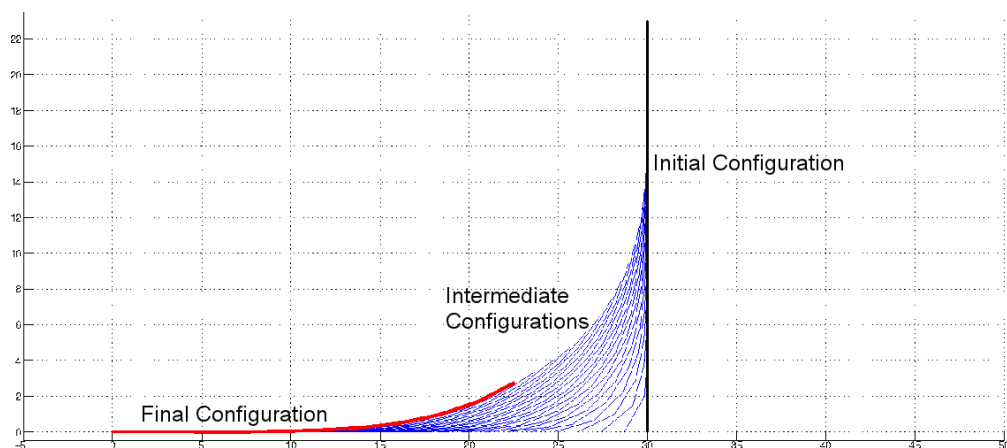


Figure 7:  $L_2$  norm minimization for a straight line

2. Rotation norm minimization introduces the notion of pure translation mode, which can be seen in the figure 8. In this case also, the motion is from right to left.
3. The third candidate norm introduced, namely the one to minimize joint rotation, introduces the rigid body behavior into the mathematical framework as can be noted from figure 9.

In the figure 9, we can notice that for the first link there is no joint rotation as there is no previous link with respect to which this can be defined. The motion of first link, in this case, has been derived using  $L_2$  norm minimization. Clearly, from the figure, we see that the whole body shows a rigid body behavior for minimal body deformation or maximum stiffness.

The distinct behavior of solutions displayed in figures 7-9 indicate the effect of objective chosen on the solution. Depending upon the nature of the problem in hand, proper objective needs to be chosen. For example, if the application is for a flexible robotic manipulator chain, the main objective will be to minimize the joint rotations so as to minimize motor actuation and power consumption, in which case metric defined in Section 4.2 for minimizing joint rotations may be more appropriate. However, if the problem is concerned with trajectory planning of a locomotive pulling coaches, then the minimizing the motion or  $L_2$  norm over time is more appropriate.

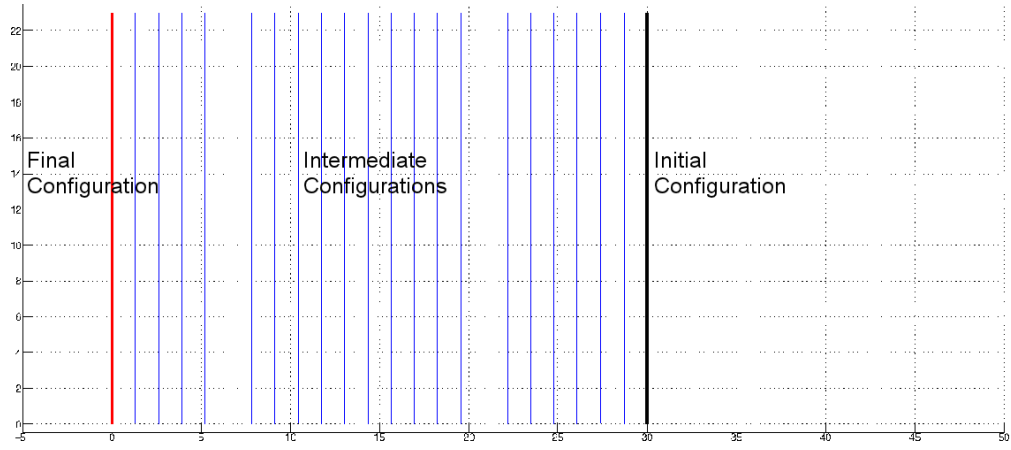


Figure 8: Rotation minimization for a straight line

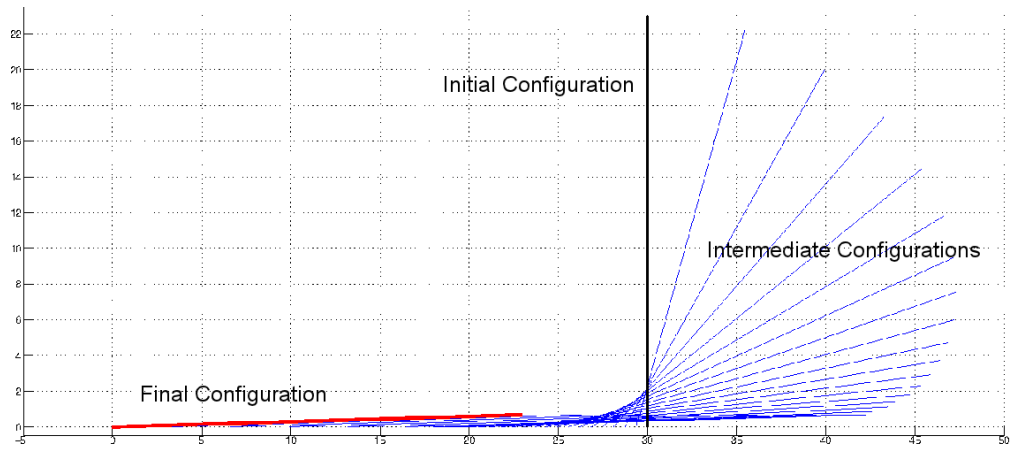


Figure 9: Joint rotation minimization for a straight line

### 5.3 Planar & spatial simulation of a generic curve subjected to generic perturbation

In this section, we present simulation and visualization of the motion of an arbitrarily chosen curve, pulled along an arbitrary path in 2D and 3D space. Three cases, namely that of an arbitrary planar curve, a parabola and a curve in 3D space are used to illustrate the features of the  $L_2$  norm minimization based schemes. In this set of simulations, we use multi-step sequential optimization.

In the planar sequential case, the input curve is discretized into 80 links of 0.05 length each and is perturbed in 250 steps of 0.075 each over a length of 8.75 units along a generic path. For overall optimization in 2D, the curve is again a parabola of the form  $y = x^2$  discretized into 20 links, each of length 0.25, and is pulled in 6 steps with average pull length 0.4 units. In the case of 3D, an arbitrary curve of length 30 is discretized into 20 links and perturbed in 2650 steps of 0.1, thus making a total pull length of 265 units.

Figure 10 shows the snapshots of the planar motion from multi-step sequential optimization and figure 11 shows planar motion of a parabola in generic direction using multi-step overall optimization. Finally, figure 12 show the snapshots of spatial motion and the accompanying videos shows the entire motion for the last two cases. It may be mentioned the length of curve, 4 and 30 units for 2D and 3D curve, remain constant during the motion. It can be clearly seen that the ‘dying-out’ property is present and this clearly leads to a more natural looking motion of the curve. One can also observe that the eventual motion of the curve aligns with the direction of the motion of the input end. It may be noted that one can see a similar “dying-out” and “aligning” motion in a ribbon being moved by a gymnast during floor exercises.

## 6 Conclusion and Future Work

This paper presents a new approach for the simulation and visualization of the motion of one-dimensional flexible objects using calculus of variations and constrained optimization. It is analytically proved that classical tractrix based solutions are direct consequence of an  $L_2$  norm minimization and minimization of the tip-velocity. Subsequently, using sequential optimization to a curve discretised by piece-wise linear segments, a much simpler and computationally more robust algorithm has been developed for the simulation of arbitrary flexible one-dimensional objects whose length is preserved during motion. It has been shown that the minimization results in a natural ‘dying out’ and aligning motion of the flexible object. An important feature of the proposed algorithm is that it is a purely *kinematics-based* solution and it does not require assuming values for mass, stiffness or damping of the flexible objects as in dynamics-based approaches. The approach can be applied to simulation and visualization of the motion of generic flexible objects such as snakes, chains, ropes etc. The proposed approach can be also used for redundancy resolution in hyper-redundant robotic manipulators.

Further, it is shown that the tractrix-based approach is one of the many possible length-preserving transformations for a smooth, arc length parametrizable curve. Through two additional candidate norms, the fact has been demonstrated that objective function chosen affects the solution drastically. Therefore, the proposed approach can give the optimized and appropriate solutions for any given functional, which in turn will be decided by the given problem.

Lack of analytical expressions for arbitrary curves and the norms have forced us to employ numerical methods. This brings along with it inherent issues, namely ones related to convergence, stability and sensitivity to initial guess in the numerical optimization procedure. Although a rigorous mathematical proof of convergence, stability and sensitivity to initial guess is not available for the theoretical approach presented in this paper, the situation is not hopeless. This is based on following specific observation and reasoning – (a) we did not face any of these issues during the numerous numerical simulations we performed on a large number of arbitrarily chosen curves pulled along arbitrary directions in 2D and 3D space, and (b) for a straight line there exists *analytical*

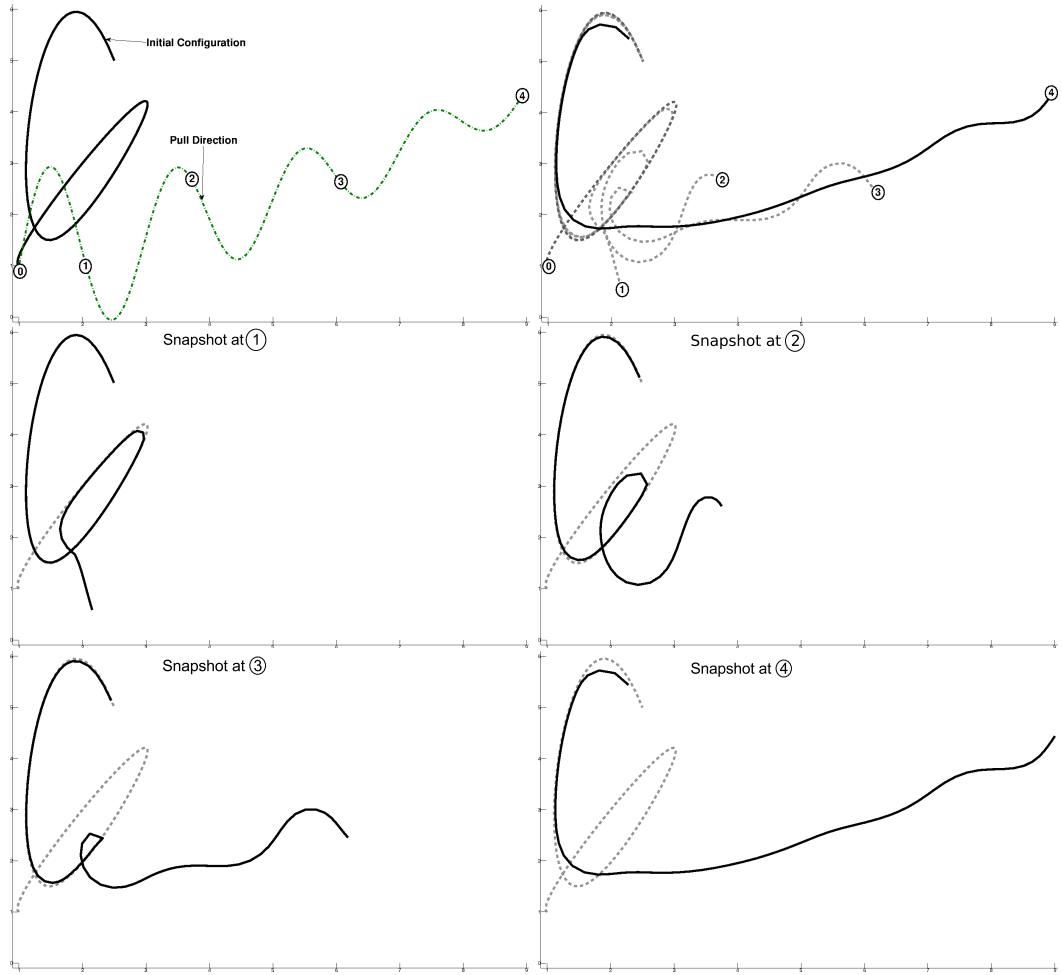


Figure 10: Multi-step sequential optimization of an arbitrary curve pulled in generic direction

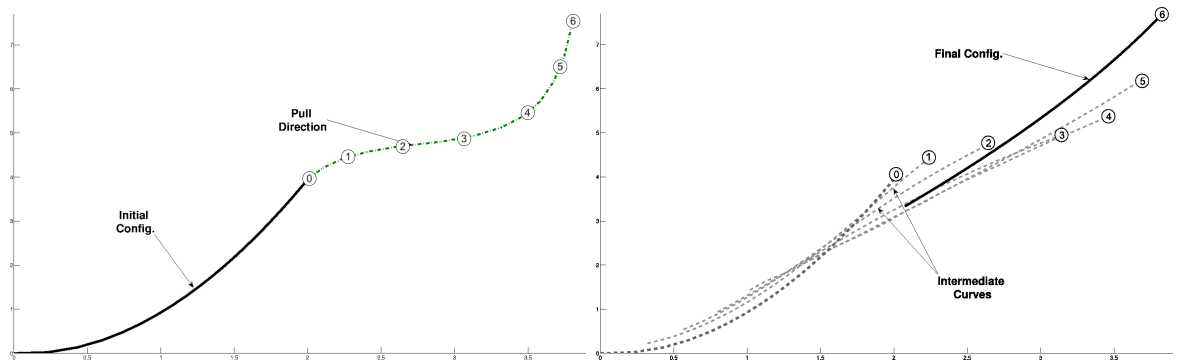


Figure 11: Multi-step overall optimization of a parabola moved along a generic direction in 2D



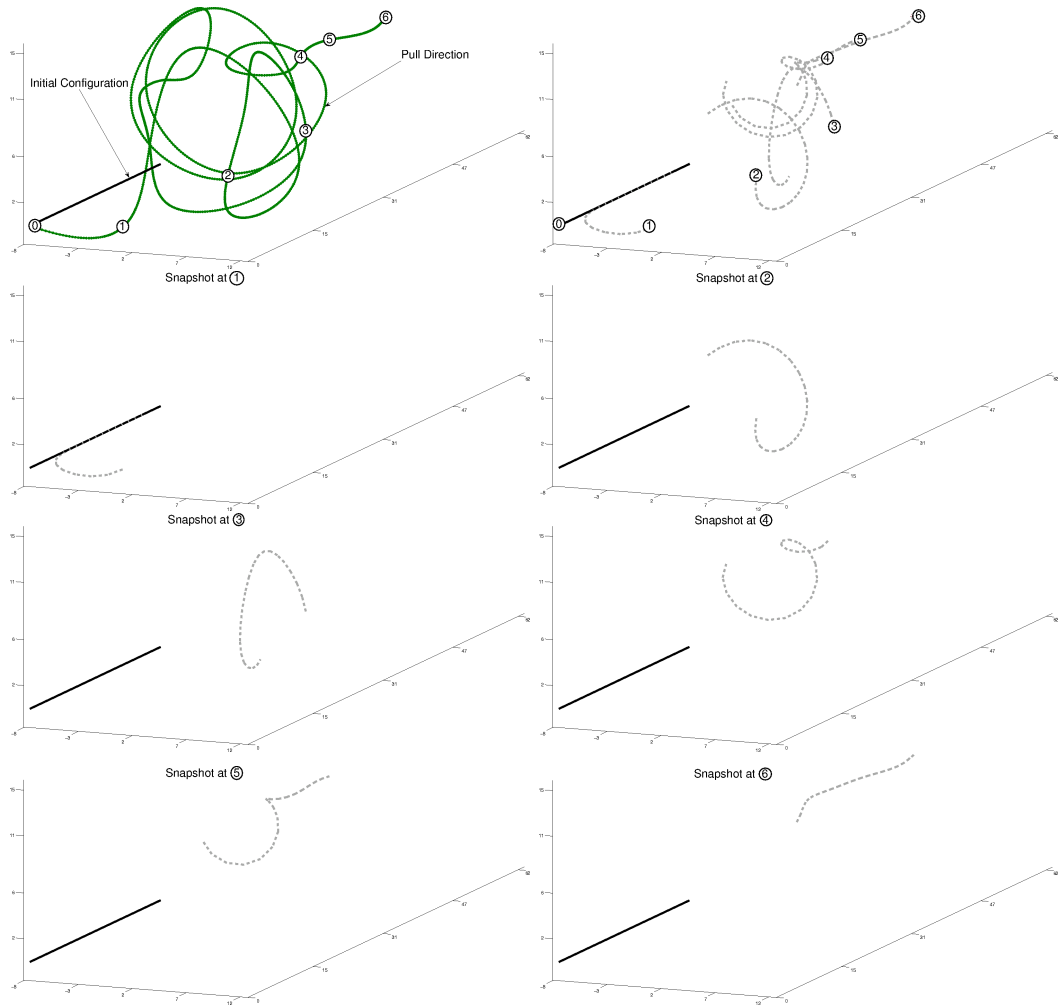


Figure 12: Multi-step sequential optimization of an arbitrary curve in generic direction in 3D

*solutions without any of the above mentioned issues* and an arbitrary curve can be considered to be the limiting case of a large number of linear segments. However, closed-form analytical expressions (as in the case of a straight line) for planar and spatial curves are expected to give more useful, qualitative insights and this is a topic of further research.

## References

- [1] Ward, K., Bertails, F., Kim, T.-Y., Marschner, S. R., Cani, M.-P. and Lin, M. C(2007) ‘A survey on hair modeling: styling, simulation, and rendering’, *IEEE Transaction on Visualization and Computer Graphics*, pp. 213-234.
- [2] Kühnapfel, U., Cakmak, H. K. and Maaß, H. (2000), ‘Endoscopic surgery training using virtual reality and deformable tissue simulation’, *Computes & Graphics*, **24**, pp. 671-682.
- [3] Kang, H. and Wen, J. T. (2002), ‘Robotic knot tying in minimally invasive surgery’, *Proc. of IEEE/RSJ, Int. Conf. on Intelligent Robots and Systems*, pp. 1421-1426.
- [4] Pai, D. K., (2002), ‘STRANDS: Interactive simulation of thin solids using Cosserat models’, *Computer Graphics Forum*, **21**, pp. 347-352.
- [5] Barzel, R., (1997), ‘Faking dynamics of ropes and springs’, *IEEE Comput. Graph. Appl.*, **17**, pp. 31-39.
- [6] Klein, C. A. and Huang, C. H. (1983), ‘Review of the pseudo-inverse for control of kinematically redundant manipulators’, *IEEE Trans. on Systems, Man, and Cybernetics*, **SMC-13**(3), pp. 245-250 .
- [7] Nakamura, Y. (1991), *Advanced Robotics: Redundancy and Optimization*, Addison-Wesley.
- [8] Liegeois, A. (1977), ‘Automatic supervisory control of the configuration and behavior of multi-body mechanisms’, *IEEE Trans., Systems, man and Cybernetics*, **7**, pp. 868-871.
- [9] Baillieul, J., Hollerbach, J. and Brockett, C. W. (1984), ‘Programming and control of kinematically redundant manipulators’, *Proc. of 23rd IEEE Conf. on Decision and Control*, pp. 768-774.
- [10] Yoshikawa, T. (1985), ‘Manipulability of robotic mechanisms’, *The Int. Journal of Robotics Research*, **4**, pp. 3-9.
- [11] Zanganeh, K. E. and Angeles, J. (1995), ‘The inverse kinematics of hyper-redundant manipulators using splines’, *Proc. IEEE Int. Conf. on Robotics and Automation*, **3**, pp. 2797-2802.
- [12] Chirikjian, G. S., Burdick, J. W. (1994), ‘A modal approach to hyper-redundant manipulator kinematics’, *IEEE Trans. on Robotics and Automation*, **10**(3), pp. 343-354.
- [13] Steinhaus, H. (1999), *Mathematical Snapshots*, 3rd ed., pp. 249-251, Dover, New York.
- [14] Reznik, D. and Lumelsky, V. (1992), ‘Motion planning with uncertainty for highly redundant kinematic structures: I. ”Free snake” motion’, *Proc. of 1992 IEEE/RSJ, Int. Conf. on Intelligent Robots and Systems*, pp. 1747-1752.
- [15] Reznik, D. and Lumelsky, V. (1993), ‘Motion planning with uncertainty for highly redundant kinematic structures: II. The case of a snake arm manipulator’, *Proc. of 1993 Int. Conf. on Robotics and Automation*, Vol. 3, pp. 889-894.

- [16] Reznik, D. and Lumelsky, V. (1994), ‘Sensor-based motion planning in three dimensions for a highly redundant snake robot’, *Advanced Robotics*, **9**, pp. 255-280.
- [17] Sreenivasan, S., Goel, P. and Ghosal, A. (2010), ‘A real-time algorithm for simulation of flexible objects and hyper-redundant manipulators’, *Mechanism and Machine Theory* **45**, pp. 454-466.
- [18] Ravi, V. C., Rakshit, S. and Ghosal, A. (2010), ‘Redundancy resolution using tractrix: Simulations and experiments’, *Trans. ASME, Journal of Mechanisms and Robotics*, **2**, pp. 1-15.
- [19] Angeles, J. (2006), ‘Is there a characteristic length of a rigid-body displacement?’, *Mechanism and Machine Theory*, **41**, pp. 884-896.
- [20] R. Weinstock, R. (1974), *Calculus of Variations: With Applications to Physics and Engineering* Dover Publications, New York.
- [21] Smith, D. (1998), *Variational Methods in Optimization*, Dover Publications, New York.
- [22] MATLAB. *version 7.12.0 (R2011a)*. The MathWorks Inc., Natick, Massachusetts, 2012.
- [23] Michael B. Monagan, Keith O. Geddes, K. Michael Heal, George Labahn, Stefan M. Vorkoetter, James McCarron, and Paul DeMarco. *Maple 14 Programming Guide*. Maplesoft, Waterloo ON, Canada, 2012.